



# Xenon isotopes in Archean and Proterozoic insoluble organic matter: A robust indicator of syngenecity?

D.V. Bekaert<sup>a,\*</sup>, M.W. Broadley<sup>a</sup>, F. Delarue<sup>b</sup>, Z. Druzhinina<sup>c</sup>, G. Paris<sup>a</sup>, F. Robert<sup>b</sup>, K. Sugitani<sup>d</sup>, B. Marty<sup>a</sup>

<sup>a</sup> Centre de Recherches Pétrographiques et Géochimiques, CRPG-CNRS, Université de Lorraine, UMR 7358, 15 rue Notre Dame des Pauvres, BP 20, 54501 Vandoeuvre-lès-Nancy, France

<sup>b</sup> IMPMC Sorbonne Universités—MNHN, UPMC Univ Paris 06, UMR CNRS 7590, IRD UMR 206, Paris, France

<sup>c</sup> California Institute of Technology, Division of Geological and Planetary Sciences, 1200 E. California Blvd, Pasadena CA91125, USA

<sup>d</sup> Department of Environmental Engineering and Architecture, Graduate School of Environmental Studies, Nagoya University, Nagoya 464-8601, Japan

## ABSTRACT

Insoluble organic materials (kerogens) isolated from ancient sedimentary rocks provide unique insights into the evolution of early life. However, establishing whether these kerogens are indeed syngenetic with the deposition of associated sedimentary host rocks, or contain contribution from episodes of secondary deposition, is not straightforward. Novel geochemical criteria are therefore required to test the syngenetic origin of Archean organic materials. On the one hand, the occurrence of mass-independent fractionation of sulphur isotopes (MIF-S) provides a tool to test the Archean origin of ancient sedimentary rocks. Determining the isotope composition of sulphur within kerogens whilst limiting the contribution from associated minerals (e.g., nano-pyrites) is however challenging. On the other hand, the Xe isotope composition of the Archean atmosphere has been shown to present enrichments in the light isotopes relative to its modern composition, together with a mono-isotopic deficit in  $^{129}\text{Xe}$ . Given that the isotopic composition of atmospheric Xe evolved through time by mass dependent fractionation (MDF) until  $\sim 2.5$  to  $2.0$  Ga, the degree of MDF of Xe isotopes trapped in kerogens could provide a time stamp for the last chemical equilibration between organic matter and the atmosphere. However, the extent to which geological processes could affect the signature of Xe trapped in ancient kerogen remains unclear. In this contribution, we present new Ar, Kr and Xe isotopic data for four kerogens isolated from 3.4 to 1.8 Gy-old cherts and confirm that Xe isotopes from the Archean atmosphere can be retained within kerogens. However, new Xe-derived model ages are lower than expected from the ages of host rocks, indicating that initially trapped Xe components were at least partially lost and/or mixed together with some Xe carried out by younger generations of organic materials, therefore complicating the Xe-based dating method. Whilst non-null  $\Delta^{33}\text{S}$  values and  $^{129}\text{Xe}$  deficits relative to modern atmosphere constitute reliable imprints from the Archean atmosphere, using Xe isotopes to provide information on the syngenetic origin of ancient organic matter appears to be a promising – but not unequivocal – tool that calls for further analytical development.

## 1. Introduction

Our understanding of the early Earth is limited by the scarcity of well-preserved ancient samples because of metamorphism and alteration (Kamber and Webb, 2001). The terrestrial rock record, which constitutes the primary source of record of primitive life, only extends to 4.0 Ga (Acasta gneisses; Bowring and Williams, 1999). Evidence for extensive water-rock interaction from the high  $\delta^{18}\text{O}$  recorded in the Jack Hills zircons can further extend the evidence for crust and oceans on Earth to 4.4 Ga (Peck et al., 2001; Wilde et al., 2001). Jack Hills zircons may as well hold the oldest evidence (4.1 Gy-old) for biogenic organic carbon, as indicated by negative  $\delta^{13}\text{C}_{\text{PDB}}$  anomalies measured from primary graphite inclusions (Bell et al., 2015). Interpreted as witness for autotrophic metabolisms such as photosynthesis, such light carbon isotope signatures were also determined in 3.95 Ga ( $\delta^{13}\text{C} \sim -25.6\text{‰}$ ; Tashiro et al., 2017) and in 3.7 Ga ( $\delta^{13}\text{C}_{\text{PDB}} \sim -19\text{‰}$ ; Rosing, 1999) early Archean rocks.

However, various abiotic processes might as well produce isotopically light organic compounds during hydrocarbon formation by kinetically controlled polymerization reactions, such as the Fischer-Tropsch reaction or abiogenic  $\text{CH}_4$  formation from  $\text{HCO}_3^-$  under hydrothermal conditions (Lollar et al., 2002; Horita, 2005). Likewise, we note that the Insoluble Organic Matter (IOM) in primitive carbonaceous meteorites is  $^{13}\text{C}$ -poor, with  $\delta^{13}\text{C}_{\text{PDB}}$  ranging from  $\approx -34$  to  $-8\text{‰}$  (Alexander et al., 2007), so some of the light carbon isotope signatures in ancient rocks could as well be inherited from extra-terrestrial precursors. This implies that the assessment of biogenicity from isotopic measurements may require combination with additional analyses (e.g., morphology, population distributions, Raman spectroscopy, and/or elemental distributions) to be valuable (Oehler and Cady, 2014). Whilst 3.8 Gyr-old banded iron formations in Isua (Greenland) may be related to the microbial oxidation of ferrous iron (Konhauser et al., 2002), positive identifications of microfossils do not extend to more than 3.5 Ga (Walter et al., 1980; Allwood et al., 2006;

\* Corresponding author.

E-mail address: [dbekaert@crpg.cnrs-nancy.fr](mailto:dbekaert@crpg.cnrs-nancy.fr) (D.V. Bekaert).

<https://doi.org/10.1016/j.precamres.2019.105505>

Received 17 August 2019; Received in revised form 15 October 2019; Accepted 16 October 2019

Available online 18 October 2019

0301-9268/ © 2019 The Authors. Published by Elsevier B.V. This is an open access article under the CC BY-NC-ND license (<http://creativecommons.org/licenses/by-nc-nd/4.0/>).

Alleon et al., 2018). Older potential remnants of life (Mojzsis et al., 1996; McKeegan et al., 2007) are still debated (van Zuilen et al., 2002; Lepland et al., 2005). Ambiguities and controversies therefore persist regarding both their biogenicity and syngenicity, with the potential for organic matter (OM) from ancient biological sources to co-exist with organic matter or reduced carbon produced by non-biologic processes, or post-depositional organic contaminants (e.g., Marshall et al., 2012).

In order to unambiguously trace the evolution of early life on Earth, it is essential to show that organic materials recovered from ancient rocks, and often regarded as potential remnants of early life, are biogenic in origin, and syngenetic in age with their host rock. Biogenicity might be inferred from morphological observations if an ancient organic structure resembles recent organic remnants that are now well accepted to be of biological origin (Westall et al., 2001). However, non-biological processes may also produce morphologies similar to biologic structures and generate misinterpretation (e.g., García-Ruiz et al., 2003; Cosmidis and Templeton, 2016). Over the past decade, in-situ 2D and 3D techniques of spectroscopy, mass-spectrometry and microscopy have been developed for evaluating organic matter characteristics at the micrometer-to-sub-micrometer-scale (see Oehler and Cady (2014), for a review). New protocols for sample collection and analysis as well as novel insights into the importance of optimal depositional settings and geologic histories for the preservation of syngenetic biomarkers have therefore been achieved. However, the potential for secondary deposition of OM, younger than the host rocks, precludes non-ambiguous determination of the age of bulk ancient organic materials.

Assessment of OM spatial relationships to surrounding minerals, veins, and fractures provides information regarding the potential occurrence of post depositional organic materials (Oehler and Cady, 2014). In particular, for an ancient organic material to be considered syngenetic with its host rock requires its compositional and structural features to be homogeneous, and indicative of a level of maturity that is consistent with that of the host rock. For instance, investigations about the elemental ratios (H/C and N/C used as proxies for organic matter preservation; Delarue et al., 2018) and spectroscopic features (Delarue et al., 2016) provide information on the effect of thermal alteration and indirectly, of the syngenicity of organic materials. The occurrence of mass-independent fractionation of sulphur isotopes can also be used to confirm, to the first order, an Archean origin of ancient sedimentary rocks and organic materials, without however providing an accurate date of formation. Determining the S isotope composition of Archean kerogens is however challenging since it requires contribution from S-bearing mineral phases (e.g., pyrites) to be eliminated or at least corrected for (Bontognali et al., 2012). The origin of early Archean pyrite records is controversial, and whether they reflect microbial activities or fractionations introduced later in the complex history of sedimentary rocks is unknown (e.g., Watanabe et al., 2009; Farquhar et al., 2000). Wacey et al. (2011) notably identified that cellular microstructures from the 3.4-billion-year-old Strelley Pool Formation (Western Australia) were associated with micrometre-sized pyrite crystals interpreted as the metabolic by-products of these cells in a multicomponent sulphur-based bacterial ecosystem.

We recently showed that the isotopic composition of Xe trapped in Archean kerogens could be used to provide model-ages for Archean organic materials (Bekaert et al., 2018). This Xe-based dating method relies on the observation that the isotopic composition of Xe in the Archean atmosphere has evolved through time by MDF (Pujol et al., 2011; Avice et al., 2018) from a precursor comprising cometary and chondritic contributions (referred to as U-Xe; Marty et al., 2017). Assuming that the evolution of Xe isotopes in the terrestrial atmosphere was a global, continuous, and protracted process, Bekaert et al. (2018) utilized literature data from quartz and barite fluid inclusions (ages and degrees of mass dependent fractionation of trapped Xe) to compute a power law evolution curve for the isotopic composition of atmospheric Xe. The analysis of Ar, Kr and Xe isotopes in kerogen MGTKS3 isolated from the 3.0 Gyr-old Farrel Quartzite (Pilbara Craton, Western Australia) revealed that the trapped Xe component was mass-dependently fractionated in favour of the

light isotopes relative to the modern day atmosphere composition, with a mono-isotopic deficit in  $^{129}\text{Xe}$ , whereas lighter noble gases (Kr isotopes,  $^{38}\text{Ar}/^{36}\text{Ar}$ ) had a modern atmosphere-like signature (Bekaert et al., 2018). Such a mono-isotopic deficit in  $^{129}\text{Xe}$  relative to the modern atmosphere composition is symptomatic of the Archean atmosphere, reflecting the fact that mantle degassing with high  $^{129}\text{Xe}/^{130}\text{Xe}$  contributed  $^{129}\text{Xe}$  (produced by the decay of extinct  $^{129}\text{I}$ ) to the atmosphere through geological periods of time (Avice et al., 2017). Thus, all observed features of Xe trapped in the Farrel Quartzite kerogen correspond to known properties of the Archean atmosphere, indicating that ancient atmospheric noble gases had been efficiently trapped and preserved over geological timescales within this sample (Bekaert et al., 2018). Reporting the degree of MDF of the trapped Xe component relative to modern atmospheric composition on the power law evolution curve of atmospheric Xe isotopic composition produced a model age of  $2.98 \pm 0.2$  Gyr for the last chemical equilibration between the kerogen and the atmosphere (Bekaert et al., 2018). These concurrent ages of the host rock (3.0 Gyr) and of Xe trapped in kerogen constitute a reliable proof of concept for the Xe-based dating method, and for its ability to produce constraints on the syngenetic origin of ancient kerogens (Bekaert et al., 2018).

The  $^{130}\text{Xe}$  enrichment factor (f) relative to  $^{36}\text{Ar}$  in kerogen MGTKS3, compared to the modern air composition [ $f = ([^{130}\text{Xe}]/[^{36}\text{Ar}])_{\text{sample}} / ([^{130}\text{Xe}]/[^{36}\text{Ar}])_{\text{ATM}}$ ], was high ( $f \sim 250$ ), in line with the efficient preservation of Xe relative to lighter noble gases (Bekaert et al., 2018). Strong retention of Xe in natural organic materials can have multiple causes, including the presence of labyrinth-with-constrictions (Torgersen et al., 2004), single-walled nanotube structures (Simonyan et al., 2001), or the presence of dangling functional groups (for example,  $-\text{COOH}$ ) inside Xe diffusion paths (Kuznetsova et al., 2000). Unusually high retention of heavy noble gases in organic materials has even been experimentally documented (Wacker et al., 1985). However, how geological processes, potentially involving thermal processing and/or multicomponent mixing, could affect the signature of Xe trapped in ancient organic materials, and potentially hamper straightforward constraints to be set on their syngenicity and relation to the host rock, remains to be explored. In this contribution, we present new Ar, Kr and Xe isotopic data for four kerogens isolated from 3.4 to 1.8 Gy-old rocks to investigate the potential for the Xe-based dating method to provide information on the post depositional history of ancient organic matter. We also developed a sample preparation and analytical procedure to analyse the S isotope composition of kerogens with limited contribution from mineral S hosted by micro-pyrites. We tested this protocol on sample kerogen MGTKS3, which, from its Xe-based model age, had been shown to be syngenetic in origin (Bekaert et al., 2018).

## 2. Materials and methods

### 2.1. Samples

All kerogens analyzed as part of the present study were isolated from Archean to Proterozoic cherts (3.5 Ga to 1.88 Ga) and have been described by Delarue et al. (2016). The host rocks underwent limited metamorphism, ranging from prehnite-pumpellyite ( $\leq 250^\circ\text{C}$ ) to greenschist facies (maximum temperature peak metamorphism of  $\sim 350^\circ\text{C} \pm 50^\circ\text{C}$ ). The Gunflint chert (hereafter PPRG134, 1.88 Gyr) was collected in the Gunflint Formation, at Port Arthur homocline (Ontario, Canada), which consists in an alternation of banded iron formations and cherts. Farrel Quartzite samples (MGTKS1 and MGTKS1up, 3.0 Gyr) were collected from the Goldsworthy greenstone belt in the Pilbara Craton (Western Australia). They originate from the same geological formation as kerogen MGTKS3 analyzed by Bekaert et al. (2018). MGTKS1up is a bedded black chert that contains microfossils (Sugitani et al., 2007, 2009; House et al., 2013 and references therein) and was most likely deposited in a shallow evaporitic basin influenced by inputs of hydrothermal fluids (Sugahara et al., 2010). The Middle Marker chert (hereafter 07SA22,  $3472 \pm 5$  Myr; Armstrong et al., 1990) corresponds to silicified detrital sediments from the

Barberton greenstone belt (South Africa; Bourbin et al., 2012). The Panorama chert (hereafter PAN1,  $3458 \pm 1.9$  Myr; Thorpe et al., 1992) is a laminated black chert sampled in the Panorama greenstone belt (Pilbara Craton, Western Australia), near the southern margin of the so-called “Trendall Ridge” (Lepot et al., 2013). It belongs to a sedimentary unit deposited in peritidal to inner platform environment (Sugitani et al., 2013). The REE + Y compositions of laterally equivalent cherts suggest precipitation from mixed marine-hydrothermal fluids (Allwood et al., 2010).

## 2.2. Noble gas analysis

Argon, krypton and xenon were extracted from kerogens by stepwise heating using a filament furnace and following the same extraction, purification and analysis procedure as described by Bekaert et al. (2018). We report here the general outlines of this method. Prior to loading the samples, each basket was degassed 3 times at  $\sim 1600^\circ\text{C}$  for 10 min in order to remove any adsorbed atmospheric noble gases. The samples were wrapped in tantalum foil and loaded into alumina-coated tungsten evaporation baskets (Ted Pella, Inc<sup>®</sup>) before baking the entire furnace at  $> 150^\circ\text{C}$  overnight under high vacuum. Kerogen aliquots, weighing between 2 and 14 mg, were heated separately over four temperature steps ( $\sim 200^\circ\text{C}$ ,  $\sim 500^\circ\text{C}$ ,  $\sim 800^\circ\text{C}$  and  $\sim 1200^\circ\text{C}$ , respectively) with Ar, Kr and Xe isotopes systematically measured on the Helix MC Plus (Thermo Fisher<sup>®</sup>) mass spectrometer. Gases released from the kerogens were first passed through an in-line Ti and Ag getter at  $650^\circ\text{C}$  to remove active gas species. Krypton and xenon were then condensed on to a quartz tube at liquid nitrogen temperature for 20 min. The quartz tube was then isolated, and the remaining Ar in the purification line was sequentially exposed to two hot ( $550^\circ\text{C}$ ; 10 min) and two cold (room temperature; 10 min) Ti getters. Argon was then admitted to the mass spectrometer and measured using peak jumping mode on faraday ( $^{40}\text{Ar}$ ) and compact dynode multiplier ( $^{36,38}\text{Ar}$ ) collectors. Krypton and xenon were then released from the quartz cold finger and purified using the same procedure as Ar. Krypton and xenon were measured using the compact dynode multiplier, with Xe isotopes being measured first, followed by the measurement of Kr isotopes on the same fraction of gas. Blanks were measured at the same temperature as the samples using a basket loaded with empty tantalum foil packets. Aliquots of standards with atmospheric isotopic compositions were analyzed each day and between each sample for subsequent spectrometer mass discrimination corrections. Errors provided for each isotopic ratio of individual measurements correspond to the quadratic sum of the internal error (standard deviation  $\sigma_{\text{int}}$  of the given isotopic ratio over the  $\sim 20$  cycles of sample analysis) and external reproducibility (standard deviation  $\sigma_{\text{ext}}$  of the given isotopic ratio over the series of standard analyses). For gas-rich samples (e.g., kerogen 07SA22), multiple analysis of the gas released at a given temperature step allowed computing standard errors ( $\sigma/\sqrt{n-1}$ , where  $n$  is the number of repeat analyses and  $\sigma$  is the standard deviation of the given isotopic ratio over the repeat analyses). Total blanks over the full range of temperatures were  $6 \times 10^{-16}$ ,  $4 \times 10^{-18}$  and  $3 \times 10^{-18}$  mol for  $^{36}\text{Ar}$ ,  $^{84}\text{Kr}$  and  $^{130}\text{Xe}$ , respectively, and had atmospheric isotopic compositions. Whereas blank contributions were potentially high for the  $400^\circ\text{C}$  and  $1100^\circ\text{C}$  temperature steps (from  $< 1\%$  up to  $50\%$ ), blank contributions associated with the release of potential trapped noble gas components at  $600^\circ\text{C}$  and  $800^\circ\text{C}$  were low,  $< 2\%$ , so no correction was applied. Blank contributions are reported in Table S1. Isotopic fractionation of Xe relative to the modern atmosphere composition (which we note FXe) was computed by error-weighted correlations following the same procedure as that of Avice et al. (2018), that is, by using the stable, non-fissiogenic, nonradiogenic  $^{126,128,130}\text{Xe}$  isotopes, in addition to  $^{131}\text{Xe}$  (only negligibly contributed by the fission of  $^{238}\text{U}$ ).

## 2.3. Sample preparation and S isotopic analysis

We analyzed three organic samples from very different geological settings for their S isotope composition. The first sample is a S-rich

organic matter from the bituminous laminites of Orbagnoux (France, upper Kimmeridgian; Mongenot et al. 1997) for which we analyzed 3 aliquots labelled r-d1 (5.8 mg), r-d2 (5.5 mg) and r-d3 (5.6 mg). These aliquots were first processed in HCl for dissolving carbonates, centrifuged and washed with MilliQ water before starting the common preparation process. The second sample corresponds to 5.0 mg of the Archean Kerogen MGTKS3 isolated from a black chert layer of the 3.0-Gy-old Farrel Quartzite (Pilbara Craton, Western Australia; Delarue et al. 2016; Bekaert et al. 2018). The third sample is 5.6 mg of Insoluble Organic Matter (IOM) from the meteorite GRO 95,502 (Grossman and Brearley, 2005).

The density of organic kerogens generally varies from  $1.1$  to  $1.35\text{ g/cm}^3$ , whilst that of pyrite, and more generally sulphides, is  $4.9 - 5.2\text{ g/cm}^3$ . Physical separation in sodium polytungstate heavy liquids ( $1.2$  to  $3.0\text{ g/cm}^3$  depending on the water to sodium polytungstate powder ratio) was therefore chosen to isolate kerogens from potential micro-pyrites and other sulphides grains. Kerogens were first placed in 14 ml plastic tubes together with 4–8 ml of sodium polytungstate. Mixtures were repeatedly agitated before leaving them to settle for 48–72 h. Floating kerogens (hereafter “light fractions”) were then collected into clean tubes. A few hours later, the powders sunk to the bottom of the plastic tubes (hereafter “heavy fractions”) were also collected into clean tubes together with 1 to 4 ml of sodium polytungstate liquid. In order to reduce the mass fraction of Na in these two separates, we sequentially diluted them with 4–12 ml of MilliQ water, agitated the mixtures and centrifuged them for 5 min at 4400 rotations per min. The liquid phase was then removed, before adding another 4–12 ml of MilliQ water and repeating the process 5–15 times depending on the sample. Residues were placed into Teflon vials and heated at  $90^\circ\text{C}$  for several hours in order to get rid of remaining water.

To extract sulfur from the light and heavy fractions of the kerogens, each residue was first mixed with 0.5 ml of hydrogen peroxide and heated in closed system for 48 h at  $90^\circ\text{C}$ . Hydrogen peroxide was then evaporated and aqua regia (1 ml) was added to each vial, before heating them in closed system for 68 h at  $150^\circ\text{C}$ . Aqua regia was then evaporated before dissolving each sample in 1 ml of MilliQ water at room temperature.

We purified the samples before analysis. We ran the samples on 0.6 ml of anionic resin Biorad AG1X8 (Paris et al., 2014). Each column with resin was rinsed with 10% V/V  $\text{HNO}_3$  ( $2 \times 10\text{CV}$ ), 33% V/V  $\text{HCl}$  ( $2 \times 10\text{CV}$ ), 0.5 N  $\text{HCl}$  ( $1 \times 10\text{CV}$ ) before loading a sample. After loading, each column was washed 5 times with MilliQ water ( $5 \times 5\text{CV}$ ) and eluted with 0.45 M  $\text{HNO}_3$  ( $3 \times 2\text{CV}$ ). Aliquots were dried down on hotplates with open lids ( $100^\circ\text{C}$ , 4 h) and diluted in 5%  $\text{HNO}_3$  and 2.5%  $\text{NaOH}$ . The samples were then analyzed on the ThermoScientific Neptune Plus MC-ICP-MS at the CRPG-CNRS using a standard-sample bracketing method (Paris et al., 2013). Samples are run at high resolution using an Aridus-II desolvating membrane to decrease oxide and hydride interferences. The plasma is run at 1000 W and data are acquired as 1 block of 50 cycles of 4.194 s each. The sequence consists of running as standard-sample-standard and measuring the instrumental blank inbetween each of them. After acquisition, raw data are processed offline using a Matlab script to identify and eliminate potential outliers (defined at the 3-sigma limit) within the fifty cycles. The sequence consists of running as standard-sample-standard and measuring the instrumental background inbetween each solution. The bracketing standard used here is a  $\text{Na}_2\text{SO}_4$  solution, itself calibrated against international standard IAEA S1 and checked against IAEA S2 and S3. After being processed on Matlab, data are corrected for instrumental fractionation, drift and background following Paris et al. (2013) using an excel spreadsheet.  $\Delta^{33}\text{S}$  is calculated as  $\delta^{33}\text{S} - 0.515 \times \delta^{34}\text{S}$  with  $\delta^{xx}\text{S} = \ln([^{xx}\text{S}/^{32}\text{S}]_{\text{sample}}/[^{xx}\text{S}/^{32}\text{S}]_{\text{V-CDT}})$ .

## 3. Results

Noble gas abundances and blank contributions are reported in Table S1. Isotope ratios for Ar, Kr and Xe are reported in Tables S2–S4, respectively. Sulphur isotopic ratios are reported in Table S5.



### 3.1. Noble gas elemental ratios.

$^{130}\text{Xe}$  enrichment factors ( $f = ([^{130}\text{Xe}]/[^{36}\text{Ar}])_{\text{sample}}/([^{130}\text{Xe}]/[^{36}\text{Ar}])_{\text{ATM}}$ ) relative to  $^{36}\text{Ar}$  and to the composition of modern air are reported in Table S1. The Gunflint kerogen (PPRG134, 1.88 Gyr), which was analyzed twice, shows the lowest  $f$  values (3 and 5, respectively), reflecting limited  $^{130}\text{Xe}$  enrichment relative to  $^{36}\text{Ar}$  and to the modern day atmospheric composition. Older samples show higher  $f$  values ( $f_{\text{PAN1}} \sim 197$ ,  $f_{075A22} \sim 194$  and  $f_{\text{MGTKS1up}} \sim 388$ ) of the same order previously found for sample MGTKS3 ( $f_{\text{MGTKS3}} \sim 250$ ; Bekaert et al., 2018). The  $f$  value for kerogen MGTKS1 is slightly higher ( $f_{\text{MGTKS1}} \sim 495$ ). Kerogen PAN1 was reanalyzed, and we found a much higher  $f$  value ( $f_{\text{PAN1b}} \sim 669$ ) potentially pointing towards a heterogeneous elemental distribution of noble gases in this sample.

Kerogen PPRG134 and 075A22 have the lowest ( $\sim 4.10^{-15} \text{ mol}^{130}\text{Xe/g}$ ) and highest ( $\sim 1.6.10^{-13} \text{ mol}^{130}\text{Xe/g}$ ) Xe concentrations, respectively, illustrating the fact that Xe concentrations in Archean kerogens can vary over orders of magnitude. The  $^{84}\text{Kr}/^{130}\text{Xe}$  of kerogens upon stepwise heating (Fig. 1) are also variable and systematically lower than the air ratio. Taken together, these results are in good agreement with heavier noble gases being preferentially trapped/preserved compared to lighter ones, in line with Xe enrichment factors observed in sedimentary rocks (Torgersen et al. 2004).

### 3.2. Argon isotope data

Argon isotopic data are reported in Table S2 and displayed on Fig. 2. Radioactive decay of  $^{40}\text{K}$  via electron capture produces  $^{40}\text{Ar}$ . A high  $^{40}\text{Ar}/^{36}\text{Ar}$  can therefore be considered as an indicator of the sample being ancient (i.e., enough time has elapsed to allow for the build-up of  $^{40}\text{Ar}$ ) and retentive for noble gases. In this framework, best samples for the Xe-based dating method would be expected to have high  $^{40}\text{Ar}/^{36}\text{Ar}$ . Sample MGTKS3#2 (Bekaert et al., 2018), given here for comparison, shows increasing  $^{40}\text{Ar}/^{36}\text{Ar}$  from 200 °C to 800 °C with a maximum  $^{40}\text{Ar}/^{36}\text{Ar}$  reaching  $2272.2 \pm 44.5$  at 800 °C. The  $^{40}\text{Ar}/^{36}\text{Ar}$  then decreases at 1200 °C towards an atmospheric-like value ( $^{40}\text{Ar}/^{36}\text{Ar}_{\text{ATM}} = 298.6$ ; Lee et al., 2006). Among all samples analyzed in the present study, only 075A22 and PAN1 reach such high  $^{40}\text{Ar}/^{36}\text{Ar}$  ratios ( $7273.8 \pm 114.5$  at 800 °C and  $3392.5 \pm 21.6$  at 500 °C, respectively). Kerogens MGTKS1 and MGTKS1up, although originating from the same geological formation as MGTKS3, exhibit maximum  $^{40}\text{Ar}/^{36}\text{Ar}$  of  $\sim 750$ . Kerogen PPRG134 shows limited excess of radiogenic  $^{40}\text{Ar}$ , with all  $^{40}\text{Ar}/^{36}\text{Ar}$  ratios being  $< 320$ . All  $^{38}\text{Ar}/^{36}\text{Ar}$  are within error of air composition (Table S2), except for sample MGTKS1up, which exhibits increasing  $^{38}\text{Ar}/^{36}\text{Ar}$  with temperature (up to  $0.2631 \pm 0.0117$  at 1200 °C)

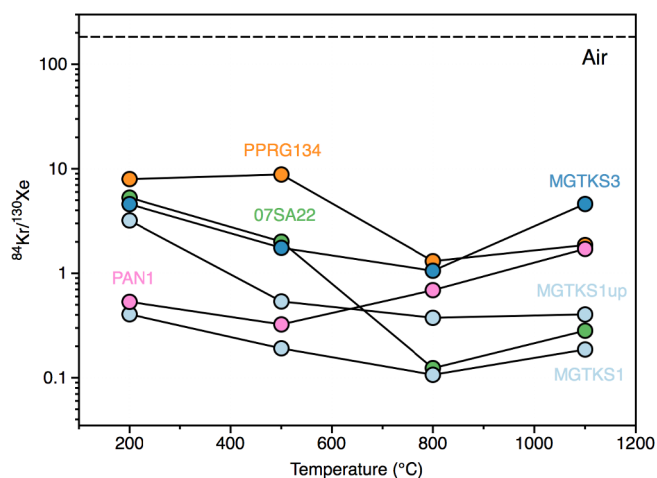


Fig. 1.  $^{84}\text{Kr}/^{130}\text{Xe}$  in Archean kerogens as a function of temperature, consistent with the preferential retention of heavier noble gases in kerogens. Air composition ( $^{84}\text{Kr}/^{130}\text{Xe} = 183$ ; Ozima and Podosek, 2002) is given for comparison.

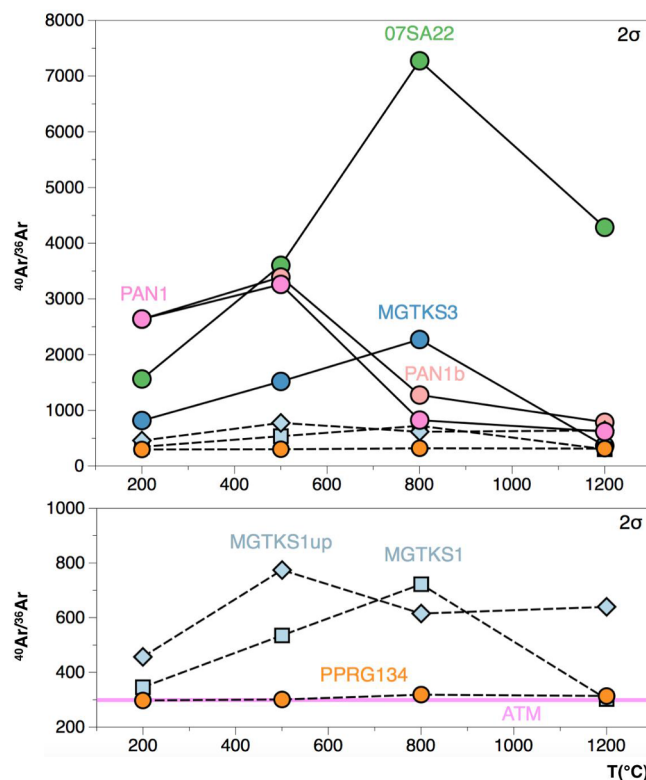
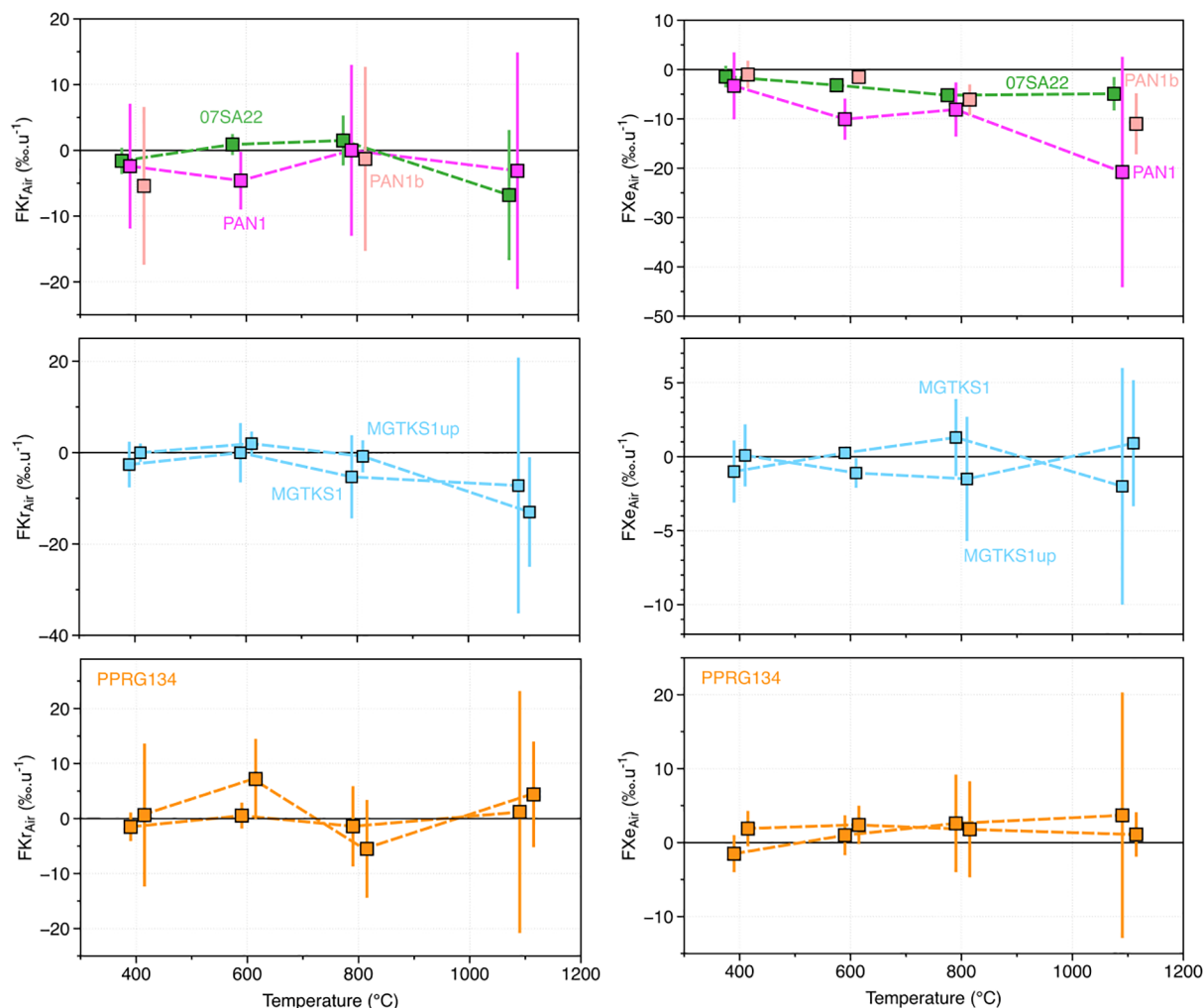


Fig. 2.  $^{40}\text{Ar}/^{36}\text{Ar}$  in Archean kerogens as a function of temperature. Among all samples analyzed here, only 075A22 and PAN1 reach  $^{40}\text{Ar}/^{36}\text{Ar}$  values comparable to that of kerogen MGTKS3, indicating they potentially preserved an ancient noble gas component. Kerogens MGTKS1 and MGTKS1up, although originating from the same geological formation as MGTKS3, exhibit lower  $^{40}\text{Ar}/^{36}\text{Ar}$  ( $\leq 750$ ), suggesting their noble gas signature may have been disrupted and, hence, they might be less suited than kerogen MGTKS3 for the Xe-based dating tool.

probably related to the release of cosmogenic noble gases trapped in residual mineral phases.

### 3.3. Krypton and xenon isotope data

Krypton and xenon isotopic compositions in kerogens are given using the delta notations normalized to  $^{84}\text{Kr}$  and  $^{130}\text{Xe}$ , respectively, and to the isotopic composition of the modern atmosphere ( $\delta^i\text{A}_{\text{air}}$  (sample) =  $(\delta^i\text{A}/\text{N})_{\text{sample}}/(\delta^i\text{A}/\text{N})_{\text{air}} - 1) \times 1000$ , where  $\text{A} = \text{Kr}$  or  $\text{Xe}$ ,  $\text{N} = ^{84}\text{Kr}$  or  $^{130}\text{Xe}$ , and  $\delta^i\text{A}_{\text{air}}$  (air) =  $\delta^i\text{Kr}_{\text{air}}$  (air) = 0‰). Degrees of MDF ( $F$ , ‰) of Kr and Xe isotopes released from the kerogens by stepwise heating are shown in Fig. 3. Apparent negative degrees of MDF for Kr at high temperature (e.g., MGTKS1up; Fig. 4) could be related to the occurrence of isobaric interferences with hydrocarbons at masses 78 ( $\text{C}_6\text{H}_6$ ) and 80 ( $\text{C}_6\text{H}_8$ ) (Fig. 4). At high temperature, cracking of the kerogen could indeed induce the production of gaseous hydrocarbons that, if not entirely purified during gas preparation, interfere with Kr light isotopes during analysis, therefore causing an overestimation of the corresponding isotopic ratios. For this reason, degrees of MDF reported Fig. 3 were computed using  $^{82}\text{Kr}/^{84}\text{Kr}$ ,  $^{83}\text{Kr}/^{84}\text{Kr}$  and  $^{86}\text{Kr}/^{84}\text{Kr}$  only. In addition, note that blank contributions at these temperatures are generally high (on the order of 50%; Table S1), supporting the idea that these signatures do not correspond to Archean atmosphere. The Kr isotopic data associated with the thermal cracking of Archean kerogens ( $\sim 400$  °C) show no significant deviation from the modern atmospheric composition, in line with previous measurements of Kr isotopes in Archean samples purported to have trapped ancient atmosphere (e.g., Pujol et al., 2011; Avicé et al., 2017, 2018; Bekaert et al. 2018),



**Fig. 3.** Degrees of mass fractionation  $F$  (‰.u<sup>-1</sup>) of Kr and Xe isotopes released from the kerogens by stepwise heating. Kr isotopic data for the Archean kerogens analyzed in the present study are similar to the modern day atmosphere composition. Xenon isotopes extracted from the kerogens are generally modern-like, except for samples PAN1 and 07SA22, which are discussed in the main text.

The Xe isotopic composition of the Gunflint kerogen PPRG134 and kerogen MGTKS1 for all heating extractions are indistinguishable from the modern atmospheric composition (Fig. 5). The presence, or not, of small isotopic deviations of Xe in kerogen MGTKS1up relative to the modern atmospheric composition is not clear (Fig. 5), and could be related to the contribution of cosmogenic Xe as suggested by increasing <sup>38</sup>Ar/<sup>36</sup>Ar with temperature (Table S2). Conversely, isotopic spectra of Xe trapped in kerogen 07SA22 consistently exhibit excesses of the light isotopes (<sup>124–129</sup>Xe) together with depletions of heavy isotopes (<sup>131–136</sup>Xe) relative to the modern atmosphere (Fig. 6). The trapped Xe components extracted at 500 °C and 800 °C are consistently mass-dependently fractionated ( $FXe_{07SA22} = -4.2 \pm 0.65\text{‰.u}^{-1}$ ). The isotopic spectrum of Xe released from kerogen PAN1 at 600 °C shows evidence for the presence of a trapped Xe component that is also mass-dependently fractionated ( $FXe_{PAN1} = -10.0 \pm 4.2\text{‰.u}^{-1}$ ), together with a mono-isotopic depletion of <sup>129</sup>Xe with respect to the mass-dependent fractionation trend (Fig. 7). Interestingly, Xe isotopes extracted at 600 °C from another aliquot of that kerogen (PAN1b) do not show any deviation from the present-day atmospheric composition, therefore pointing towards a heterogeneous composition of Xe isotopes in kerogen PAN1, in addition to the heterogeneous elemental distribution of noble gases in that sample as reported here above (Fig. 7). At last, once corrected for mass dependent fractionation relative to a starting composition similar to U-Xe, the <sup>131–136</sup>Xe excesses observed for kerogens 07SA22 and PAN1 are compatible with the presence of products of the spontaneous fission of <sup>238</sup>U -

and not <sup>244</sup>Pu - as commonly observed for Archean sedimentary rocks (Fig. 8; Avice et al., 2017; Bekaert et al., 2018).

#### 3.4. Sulphur isotope data

The S isotopic signatures of light and heavy separates from kerogen MGTKS3 are distinct from the modern atmosphere composition, with positive anomalies in  $\Delta^{33}\text{S}$  and  $\delta^{34}\text{S}$  (Fig. 9). Conversely, the Orbagnoux and GRO 95502 kerogens display close to zero  $\Delta^{33}\text{S}$  values, with negative and positive  $\delta^{34}\text{S}$  values, respectively (Fig. 9). Slightly negative  $\delta^{34}\text{S}$  for the Orbagnoux samples are in agreement with values attributed to the microbial reduction of sulfates (Shen et al. 2009), and slightly positive  $\delta^{34}\text{S}$  for the GRO 95502 IOM also fall within the range of previously reported values for extraterrestrial materials (Gao and Thieme, 1993a,b).

### 4. Discussion

#### 4.1. A Xe-based dating-tool for ancient organic matter.

An Archean atmospheric Xe signature associated with syngenetic organic matter corresponds to excesses of the light isotopes (<sup>124–129</sup>Xe) together with depletions of heavy isotopes (<sup>131–136</sup>Xe) relative to the modern atmosphere, with a possible mono-depletion in <sup>129</sup>Xe (Avice et al., 2017). The isotopic evolution of atmospheric Xe through

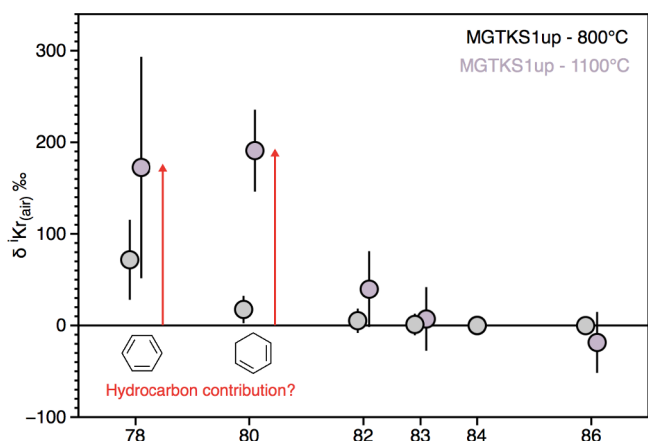


**Fig. 4.** Kr isotopic spectrum of kerogen MGTKS1up at 800 °C and 1100 °C, normalized to air composition. Although the light isotopes ( $^{78,80}\text{Kr}/^{84}\text{Kr}$ ) appear to be in excess relative to the atmospheric composition,  $^{86}\text{Kr}/^{84}\text{Kr}$  present no apparent deficits. At high temperature, cracking of the kerogen might induce the production of gaseous hydrocarbons that, if not entirely purified during gas preparation, could interfere with Kr light isotopes (e.g., benzene for  $^{78}\text{Kr}$ ,  $\text{C}_6\text{H}_8$  for  $^{80}\text{Kr}$ ) during analysis, therefore causing an overestimation of the corresponding isotopic ratios. This could notably induce a potential bias in the determination of Kr degree of MDF. For this reason, degrees of Kr MDF (Fig. 3) were computed using  $^{82}\text{Kr}/^{84}\text{Kr}$ ,  $^{83}\text{Kr}/^{84}\text{Kr}$  and  $^{86}\text{Kr}/^{84}\text{Kr}$  only.

geological times recently attracted broad interest, notably for setting time constraints on the history of surface volatile regassing into the mantle (e.g., Parai and Mukhopadhyay, 2018; Péron and Moreira, 2018). Although the exact driving mechanism behind this isotopic evolution remains debated (Hébrard and Marty, 2014; Zahnle et al., 2019), the MDF of U-Xe towards modern atmospheric values could have resulted from Xe ion-escape to space, a process that can also account for the depletion of Xe in air relative to other noble gases (see Bekaert et al., 2018 for more details). Although recently developed 1-D models of hydrodynamic diffusion-limited hydrogen escape from highly-irradiated  $\text{CO}_2\text{-H}_2\text{-H}$  atmospheres (Zahnle et al., 2019) concluded for the ion-escape model to provide the best explanation for Xe's protracted fractionation, at least one additional feature (e.g., limiting escape to narrow polar windows, or limiting Xe escape to brief episodes) is required to make the ion-escape model work over two billion years. Further work is therefore needed to elucidate on the exact conditions accounting for the progressive Xe MDF in the Archean atmosphere. Uncertainties regarding the driving mechanism behind this isotopic evolution do not however preclude the use of Xe isotopes as a paleo-chronometer. New data from Avice et al. (2018) support the choice of the power law evolution curve defined by Bekaert et al. (2018) as a good proxy for Xe isotopic evolution in the Archean atmosphere (Fig. 10), except for one data point (Fortescue Group, Hamersley Basin, Australia; 2.7 Ga, reported in light grey Fig. 10). This data point leaves the potential for the evolution of atmospheric Xe isotopes to have been discontinuous, but further work is needed to confirm this possibility.

The Xe-based dating method for ancient organic matter also relies on the potential for ancient organic materials to trap and preserve significant amounts of Xe from the Archean atmosphere. The syngenetic origin of organic material cracking below 350 °C is highly disputable since it can originate from several post-deposition contaminations and/or from residual bitumen (soluble fraction of organic matter) for which syngenecity is still an open issue (French et al., 2015). Using Rock-Eval Pyrolysis, thermal cracking of syngenetic Archean kerogens occurs at between 450 and 586 °C (Spangenberg and Frimmel, 2001; Delarue et al., 2018), as observed for kerogens MGTKS3 (Bekaert et al., 2018). Noble gases released in the 400–600 °C range (i.e. at ~500 °C in the present study) for these samples would therefore be closely related to the cracking of a syngenetic and thermorecalcitrant component.

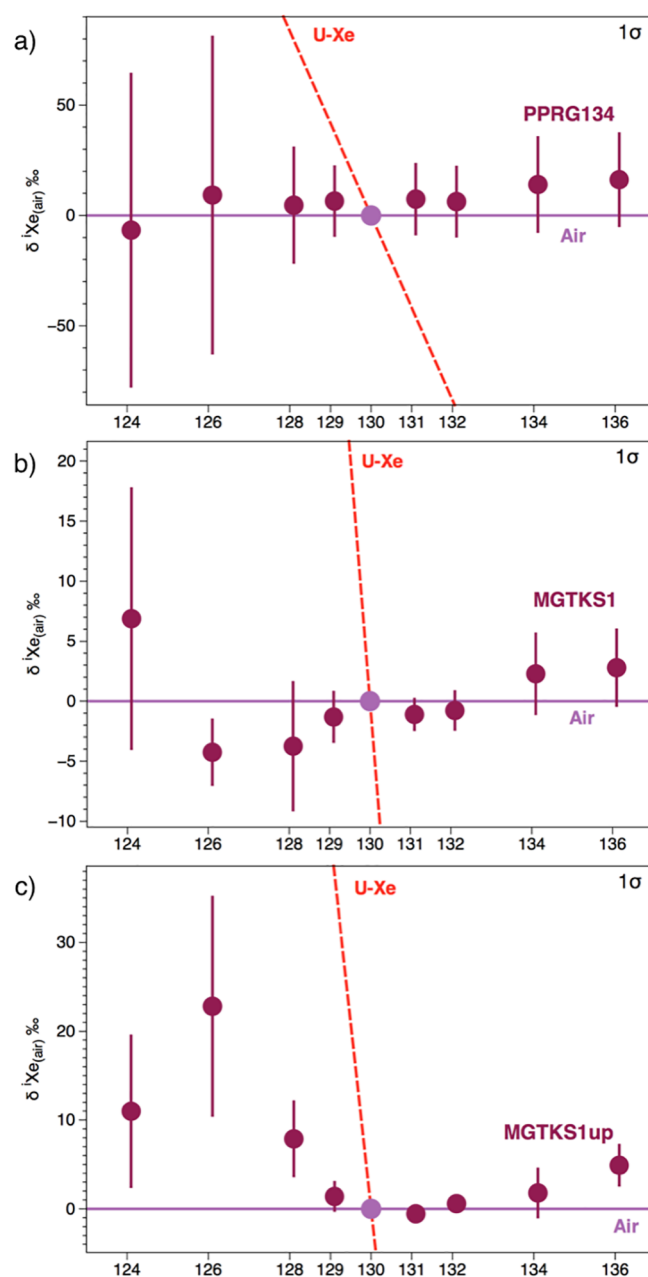


**Fig. 5.** Xe isotopic spectra of the trapped noble gas component in kerogen PPRG134 (a), MGTKS1 (b) and MGTKS1up (c), normalized to  $^{130}\text{Xe}$  and to the modern atmosphere composition (Ozima and Podosek, 2002). Error bars are  $1\sigma$ . The degree of MDF of U-Xe relative to modern atmosphere is given as a red dashed line for comparison. (For interpretation of the references to colour in this figure legend, the reader is referred to the web version of this article.)

To date, the most recent identification of ancient atmosphere has been proposed for mine fluids younger than 1.85 Ga (Warr et al., 2018). The youngest sample analyzed as part of the present study (1.88 Gyr old, kerogen PPRG134) has a Xe isotope composition that is indistinguishable from that of the modern atmosphere, in agreement with modern-like isotope compositions of the atmosphere being reached ~2 Ga (Bekaert et al., 2018). Sample PPRG134 released only limited amounts of Xe, implying that, if more material could be analyzed, a sufficient level of precision could be reached, allowing potential deviations from the modern atmospheric composition to be detected. In kerogen PPRG134, the low noble gas concentrations and very low  $^{130}\text{Xe}$  enrichment factors relative to  $^{36}\text{Ar}$  and to the composition of modern air (Table S1) might however indicate that noble gases released from

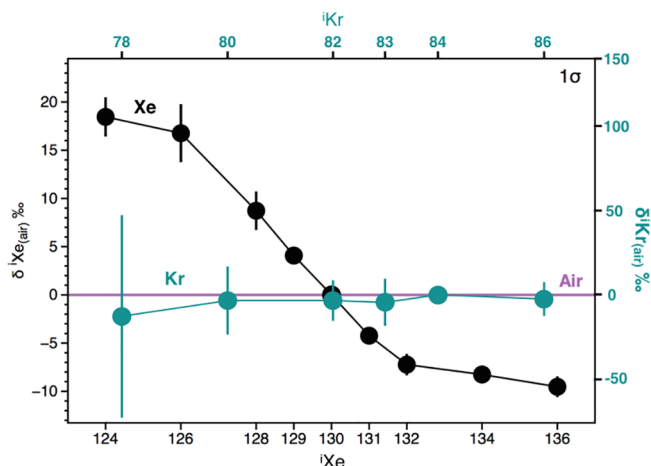


Fig. 6. Kr and Xe isotopic spectra of the trapped noble gas component in kerogen 07SA22, normalized to  $^{84}\text{Kr}$  and  $^{130}\text{Xe}$ , respectively, and to the modern atmosphere composition (Ozima and Podosek, 2002). Error bars are  $1\sigma$ .

that sample correspond to adsorbed modern air (Wacker, 1989, Marrocchi and Marty, 2013), with no evidence for the occurrence of an ancient trapped Xe component.

Kerogens 07SA22 and PAN1 show evidence for ancient atmospheric Xe components akin to the one observed in kerogen MGTKS3 (Bekaert et al., 2018). However, as illustrated in Fig. 10, the degrees of MDF of trapped Xe within kerogens 07SA22 ( $\text{FXe}_{07\text{SA}22} = -4.2 \pm 0.65\text{‰} \cdot \text{u}^{-1}$ ) and PAN1 ( $\text{FXe}_{\text{PAN1}} = -10.0 \pm 4.2\text{‰} \cdot \text{u}^{-1}$ ) produce model ages ( $2.32^{+0.10}_{-0.11}$  and  $2.99^{+0.33}_{-0.44}$  Gyr-old, respectively) that are lower than those of the corresponding host rocks ( $3472 \pm 5$  Myr and  $3458 \pm 1.9$  Myr, respectively; Armstrong et al., 1990; Thorpe et al., 1992) at the one sigma-level. At the two-sigma level, model ages for kerogens 07SA22 and PAN1 are  $2.32^{+0.19}_{-0.22}$  and  $2.99^{+0.59}_{-1.24}$  Gyr-old, respectively. Given the large uncertainty associated with the model age of kerogen PAN1, it potentially overlaps with the actual age of the host rock at the two-sigma level, although this clearly does not constitute a good match. For the rest of the discussion, the model age for kerogen PAN1 is therefore considered to be lower than that of its host rocks. Variable noble gas concentrations from one kerogen to another possibly reflect differences in the depositional environments of the host rocks, or variable efficiencies at trapping and/or preserving noble gases within organic materials. The next sections discuss the potential mechanisms accounting for lowering the degree of

MDF of trapped Xe components during the post-depositional evolution of organic matter, including mixing with a more recent Xe-bearing organic generation and diffusive loss during thermal metamorphism or aqueous alteration.

#### 4.2. Multi-component mixing

The low porosity of cherts is commonly advocated for making the syngenetic organic matter less prone to postdepositional contamination (Derenne et al., 2008). However, Raman spectroscopic data collected on the organic material present within the matrix of the Apex chert, one of the most well studied Archean deposits (e.g., Schopf, 1993; De Gregorio and Sharp, 2006), indicated the presence of two different phases of carbonaceous materials deposited as separate phases in the quartz matrix (Marshall et al., 2012). Hence, several generations of organic materials, of variable ages, could potentially coexist within a given kerogen. In this case, the final degree of MDF of the total trapped Xe component can be formulated as:

$$\delta\text{Xe}_{\text{Tot}} = \sum_{i=1}^n f_i * \text{FXe}_i * [\text{Xe}]_i$$

where  $\delta\text{Xe}_{\text{Tot}}$  is the degree of MDF of the total trapped Xe component,  $n$  is the number of coexisting generations of organic materials,  $f_i$  is the mass fraction of organic generation  $i$ , and  $\text{FXe}_i$  and  $[\text{Xe}]_i$  are the degree of MDF and concentration of Xe associated with organic generation  $i$ , respectively. Accordingly, the weight a given generation of organic materials (with a given  $\text{FXe}$ ) will have on the Xe isotopic signature of the total kerogen relies on both its mass fraction and Xe concentration. This implies that a generation of organic materials contributing limitedly to the total mass of the sample could have a significant effect on the final signature of the trapped Xe component if its Xe concentration were high. Conversely, an organic component carrying negligible amounts of Xe would have little influence on the final signature of the trapped Xe component, even at high mass fraction. This points towards a potential decoupling between the isotopic signature of the total Xe trapped component and the mass fractions of organic generations within a given kerogen. In addition, during isolation of organic materials from their host rocks, acid treatment with HF/HCl might induce the formation of neo-formed minerals such as fluorides (Garcette-Lepcq et al., 2000), which have to be removed before analysis of the Xe isotopes. These minerals would likely carry noble gases with modern atmosphere-like isotopic compositions, therefore inducing a potential

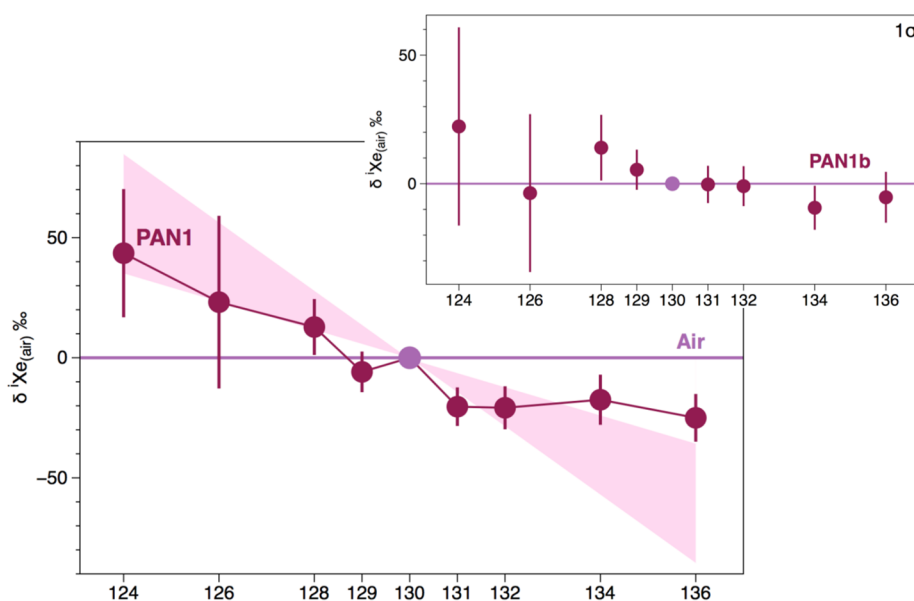


Fig. 7. Xe isotopic spectrum of the trapped noble gas component in kerogen PAN1 normalized to  $^{130}\text{Xe}$  and to the modern atmosphere composition (Ozima and Podosek, 2002). The shaded area represents the uncertainties associated with the degree of MDF computed from the Xe isotopic spectrum of the kerogen PAN1. The Xe isotope spectrum of PAN1b is given for comparison. Error bars are  $1\sigma$ .



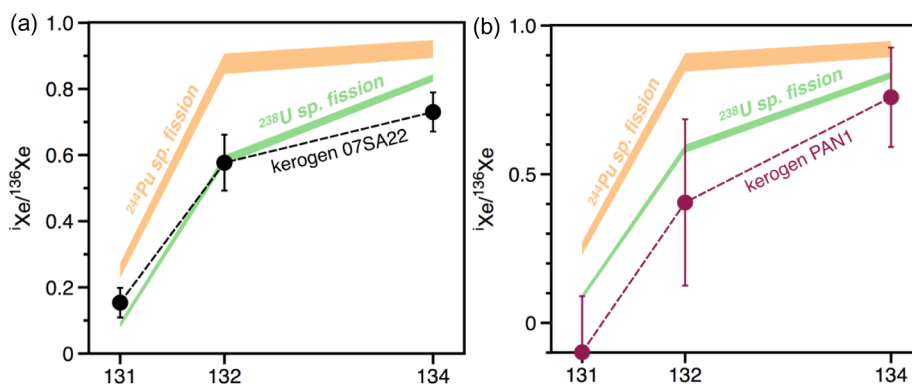


Fig. 8. Xenon fission spectra of kerogens 07SA22 (a) and PAN1 (b) corrected for mass dependent fractionation relative to a starting isotopic composition similar to U-Xe. Both spectra are in better agreement with spontaneous fission from  $^{238}\text{U}$  and not  $^{244}\text{Pu}$ . Fission spectra are from Porcelli and Ballentine (2002).

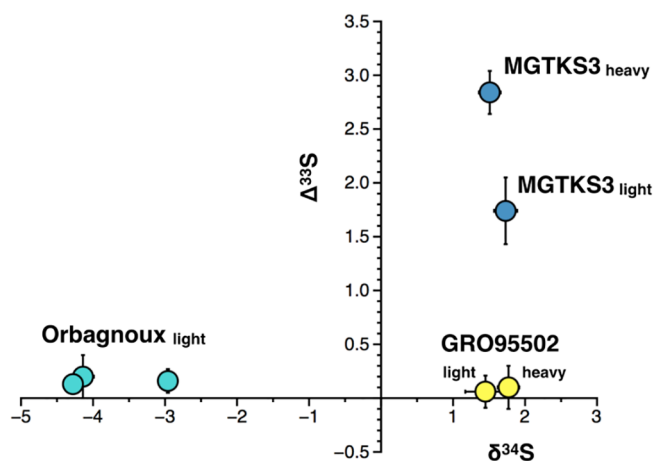


Fig. 9. Sulphur isotope composition of the S-rich organic matter from the bituminous laminites of Orbagnoux (France, upper Kimmeridgian; Mongenot et al., 1997; 3 aliquots), the Archean Kerogen MGTKS3 isolated from a black chert layer of the 3.0-Gy-old Farrel Quartzite (Pilbara Craton, Western Australia; Delarue et al., 2016; Bekaert et al., 2018), and IOM from the meteorite GRO 95,502 (Grossman and Brearley, 2005). The “light” and “heavy” fractions refer to the residues after separation in heavy liquid.

bias in the determination of the degree of MDF of the Xe trapped component if they were to still be present to some extent in the final kerogen.

Whilst the occurrence of mass-dependently fractionated Xe confirms the presence of Archean atmospheric Xe within the organic component (provided that lighter noble gases – e.g.,  $^{38}\text{Ar}/^{36}\text{Ar}$ , Kr isotopes – are not fractionated), only a good match between the Xe-based age and that of the host rock warrants the presence of a syngenetic organic component. If the degree of Xe MDF is lower than expected from the age of the host rock, no firm conclusion based on Xe isotopes solely can be drawn regarding the presence/absence of a syngenetic component. Indeed, such a signature could be accounted for by (i) mixing of a syngenetic component with a younger generation of organic materials that lowers the degree of MDF of the total Xe, or by (ii) the absence of a syngenetic component but occurrence of a unique generation of organic materials that is younger than the host rock. In case of a post-depositional organic contribution, assessment of organic matter spatial relationships to surrounding minerals, veins, and fractures, as well as comparison between Raman spectra determined on kerogens, on the mineral matrix, and on secondary hydrothermal veins (e.g., Marshall et al., 2012; Bekaert et al., 2018) can provide information regarding the multiplicity of organic sources.

The potential for multiple generations of CM to coexist in Archean kerogens illustrates the difficulty of searching for signs of life in Archean rocks. Rock-Eval pyrolysis of isolated OM from several Archean samples

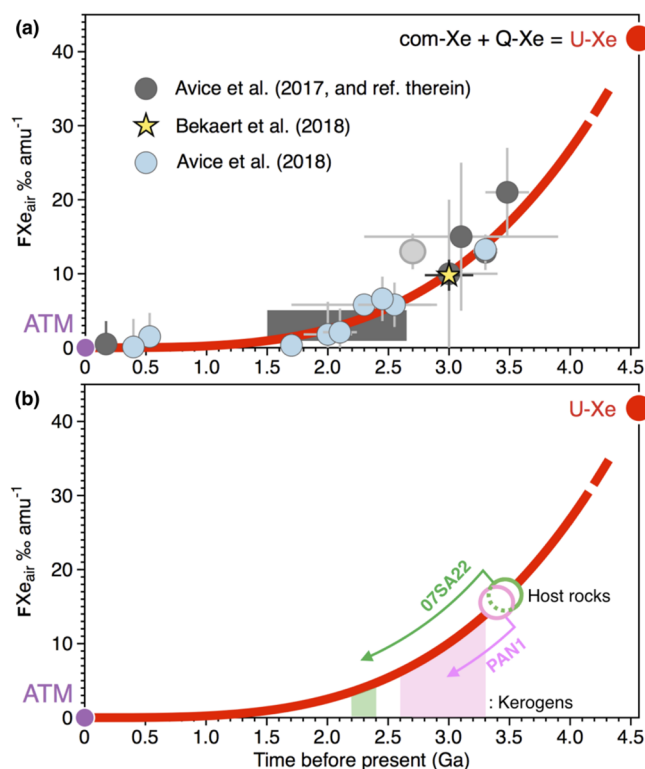


Fig. 10. MDF of atmospheric Xe with time relative to modern atmosphere (FXe). The red curve corresponds to the power law evolution ( $y = 0.238 \times x^{3.41}$ ) computed by Bekaert et al. (2018) from data reported in Avicé et al. (2017). (a) Novel data (Avicé et al., 2018; reported at 2σ) support the use of this evolution curve, with however one “anomalous” point at 2.7 Ga (Fortescue Group, Hamersley Basin, Australia), reported here in light grey. (b) Two kerogens analyzed as part of this study (PAN1 and 07SA22) show the occurrence of ancient atmospheric Xe. However, the corresponding ages derived from Xe evolution curves (vertical shaded regions beneath the curve, with uncertainties at 1σ) are systematically lower than ages of the respective host rocks (open circles). The lowering of the MDF of the trapped Xe component relative to modern atmosphere might be interpreted in terms of post-depositional history of the related kerogens. (For interpretation of the references to colour in this figure legend, the reader is referred to the web version of this article.)

(Delarue et al., 2018) revealed the co-occurrence of various OM pools characterized by different thermal stabilities. Seven out of ten isolated Archean OM samples analyzed by Delarue et al. (2018) were characterized by the release of hydrocarbons in a narrow pyrolysis temperature range (576–586 °C) corresponding to the thermal cleavage of kerogen-bound hydrocarbon. However, multiple generations of hydrocarbons upon pyrolysis have also been observed in the MGTKS1up and



MGTKS3 isolated OM (Delarue et al., 2018), pointing towards the existence of several distinct pools of OM generating hydrocarbons at high pyrolysis temperature. The occurrence of distinct pools of OM does not necessarily indicate the presence of distinct generations and, in the case of multiple generations of hydrocarbons, attributing a given Xe signature to a particular generation of OM appears unrealistic. Measuring the Xe isotopic composition of individual organic microstructures would require a high sensitivity that cannot be achieved using conventional static mass spectrometry. A promising avenue of investigation could be to couple *in situ* laser ablation techniques with an ultrasensitive, resonance ionization mass spectrometry (Gilmour and Turner, 1994).

#### 4.3. Xenon mobility in organic materials

This section investigates the possibility for a syngenetic organic component to have lost – at least part of – its initially trapped Xe. Anomalous adsorption of heavy noble gases onto surface-associated defects, including those of mineral phases, has been experimentally documented (e.g., Yang et al., 1982). The mechanisms accounting for efficient trapping and preservation of atmospheric gases, especially Xe into organic materials, are not fully understood, but do not yield measurable isotopic fractionation without ionization ( $-0.18‰ \pm 0.08‰$ ; Marrocchi and Marty, 2013). Elemental ratios and corresponding *f* factors indicate preferential incorporation and/or retention of Xe over lighter noble gases into organic materials. The natural occurrence of obstacles inside Xe's diffusion paths could delay/prevent its mobility within the organic matrix constrictions, therefore causing its preferential retention with respect to lighter noble gases (Kuznetsova et al., 2000). As we find in the present study, Xe concentrations in kerogens is highly variable, potentially reflecting differences in Xe concentrations within the depositional environments of the host rocks, or variable efficiencies at trapping and/or preserving noble gases over geological periods of time. Note that trapping of Xe atoms in organics does not yield measurable isotopic fractionation without ionization (Marrocchi and Marty, 2013). Under ionizing conditions, Xe trapping onto solids would favour the heavy isotopes (Marrocchi and Marty, 2013; Kuga et al., 2015) and not the light ones as observed here.

The very low diffusion coefficients for Xe resulting from its large radius, the structural changes of organic matter during carbonization (e.g. polyaromatic layer stacking), and the establishment of a closed system during silicification, would contribute together to preserving Xe in Archean kerogens over geological periods of time. One possibility is that a critical temperature (activation energy) has to be reached to allow Xe atoms to become mobile (e.g. if Xe is encapsulated in a cage-like molecular structure that would only be damaged at a high enough temperature). This has been studied in the framework of noble gas trapping in/releasing from fullerenes (C<sub>60</sub> and larger), which present a closed central cavity that is large enough to accommodate noble gas atoms (including Xe; Saunders et al., 1996). Fullerenes are remarkably stable since several C–C bonds must be broken for the noble gas atoms to escape. Likewise, the loss of an initially trapped Xe component through cracking of the kerogen would indicate that the structure of the organic material has been modified, and that it is not retentive for Xe anymore. In this framework, a scenario where a syngenetic organic component would have lost its initially trapped Xe, which was then replaced by younger atmospheric Xe incorporated into the organic materials at a time corresponding to the Xe-based model age, would be unlikely.

Preferential loss of the lightest isotopes over to the heaviest ones during partial loss of an initially trapped Xe component could cause artificial decrease in the absolute degree of Xe MDF with respect to the modern atmosphere composition, therefore yielding underestimated Xe-based model ages. However, no sample has been found to exhibit a positive degree of MDF relative to the modern atmosphere composition, indicating that if this process was for instance the cause of null FXe in MGTKS1, increase in the degree of Xe MDF toward zero would have been coincidentally stopped at modern atmospheric composition.

Likewise, diffusive loss should necessarily affect all noble gases in such a way that, if Xe isotopes were to have been fractionated during partial loss, then Kr isotopes should also be fractionated to at least the same extent, or more for a mass-dependent process, which is not observed. This is also valid for potential mass fractionation effects during the sample's maturation and/or partial filling/emptying of the sample's porosity by secondary fluid circulations (Torgersen et al., 2004). In addition, preferential loss of the lightest isotopes over to the heaviest ones during partial loss should yield a Xe component released at high temperature being enriched in the heaviest isotopes over to the lightest ones, which is never observed. All kerogens investigated in the present study show degrees of metamorphism that range from prehnite-pumpellyite to greenschist facies (Delarue et al., 2016), indicating the metamorphism maximum temperature did not exceed ~350 °C. Although samples were therefore held at 350 °C for potentially significant periods of time, trapped Xe components expected to be released within the 400–600 °C temperature window could have been limitedly affected. At last, kerogens MGTKS3 (Bekaert et al., 2018) and MGTKS1(up) originate from the same geological formation and were spatially separated by only a few tens of centimetres in the stratigraphic column (Delarue et al., 2016). One can therefore consider that they experienced similar thermal histories. Yet, it appears that kerogen MGTKS3 efficiently preserved its original trapped Xe component, whereas kerogen MGTKS1 and MGTKS1up lost their potential syngenetic Xe component.

Taken together, these considerations suggest that partial diffusive loss of an initially trapped, syngenetic Xe component during thermal metamorphism is unlikely to cause the observed lowering of Xe's degree of MDF relative to the modern atmosphere composition. Based on our noble gas data, we propose that mixing with younger generation(s) of organic material, with or without loss of an initial, syngenetic component, and/or contribution from neo-formed minerals alike to fluorides carrying atmospheric noble gases, would be the two most likely processes accounting for Xe-based model ages being lower than expected from the ages of the host rocks. Differences in the Xe isotope composition of samples originating from the same stratigraphic column may therefore arise from variable abilities at locally preserving closed systems and hampering mixing with more recent generations of organic materials. More work is however needed to better understand the mechanisms controlling Xe incorporation and mobility within kerogens.

#### 4.4. Archean kerogens and early life: dating tools

The occurrence of mass-independently fractionated sulphur isotopes (MIF-S) can be used to confirm the Archean origin of ancient sedimentary rocks and potentially organic materials (e.g., Farquhar et al., 2000; Bontognali et al., 2012). The presence of MIF-S in sedimentary rocks older than ~2.4 Gyr, and the absence of MIF-S in younger rocks, has been considered the best evidence for a dramatic change from an anoxic to oxic atmosphere around 2.4 Gyr ago (e.g., Farquhar et al., 2000; Pavlov and Kasting, 2002). Reactions between reduced inorganic S and organic compounds are thought to substantially enhance the stabilization and burial of OM in anoxic environments (Boussafir et al., 1995; Damsté and De Leeuw, 1990), but the sulfurization process is poorly understood. Under certain conditions, S can be incorporated into OM on a timescale of days (Raven et al., 2016). In addition, determining the S isotope composition of Archean kerogens, excluding significant contribution from associated S-bearing mineral phases, is extremely challenging (Bontognali et al., 2012). Using our newly developed protocol to specifically separate by density kerogens (light fraction) from S-bearing minerals (concentrated in the heavy fraction), we find that, contrary to the extra-terrestrial IOM (GRO 95502) or the modern kerogen Orbagnoux, archean kerogen MGTKS3 has a positive MIF-S signature ( $\Delta^{33}\text{S} = 2.84 \pm 0.20$  and  $1.74 \pm 0.31$  for the heavy and light fractions, respectively) therefore supporting its Archean origin (> 2.4 Gyr). Although we cannot exclude that residual micro- to nanopyrates still contribute to the S isotope composition determined for the

light fraction of the kerogen, this new data confirms that it is possible to measure Xe with an Archean signature (Bekaert et al., 2018) in kerogens with Archean geochemical characteristics. Sulphur isotopes do not however constitute a definitive tool for providing model ages of Archean kerogen and testing their syngenetic origin.

Relative to cosmochemical precursors (solar or chondritic), atmospheric xenon presents a mono-isotopic excess of  $^{129}\text{Xe}$  produced by the decay of extinct  $^{129}\text{I}$  (Ozima and Podosek, 2002). This excess was mainly acquired during the Earth's formation and early evolution (Marty et al., 2017) but mantle degassing has also contributed  $^{129}\text{Xe}$  to the atmosphere through geological time, most likely in a relatively short ( $\approx 300$  Myr) burst of mantle activity at the end of the Neo-Archean (Marty et al., in press). Trapped Archean atmospheric xenon shows a mono-isotopic excess of  $^{129}\text{Xe}$  that is slightly less pronounced than in the present atmosphere (Avice et al., 2018; Marty et al., in press). The presence of a mono-isotopic deficit in  $^{129}\text{Xe}$  is therefore symptomatic of the Archean atmosphere, prior to  $\sim 2.3$  Ga (Marty et al., in press). The  $^{129}\text{Xe}$  mono-isotopic deficit in kerogen PAN1 lends further credence to the conclusion of an Archean organic matter component being present in this sample. The absence of a  $^{129}\text{Xe}$  mono-isotopic deficit and occurrence of a MDF signature in kerogen 07SA22 might indicate that influx of mantle-derived  $^{129}\text{Xe}$  to the atmosphere was completed prior to the cessation of MDF of Xe isotopes in the atmosphere. According to the degree of MDF of Xe in 07SA22 relative to modern atmosphere ( $-4.2 \pm 0.65\text{‰.u}^{-1}$ ), the last chemical equilibration of the kerogen with the atmosphere could have occurred  $2.3 \pm 0.1$  Ga. We speculate that the observation of a  $^{129}\text{Xe}$  mono-isotopic deficit in ancient kerogens could also be used as  $\Delta^{33}\text{S}$  values, to infer the presence of a trapped Archean Xe component.

As illustrated in the present study, the Xe-based dating tool for Archean kerogens requires conditions (kerogen homogeneity, uniqueness of the organic source, efficient preservation and non-disruption of the initially trapped Xe component) that may not be the rule in nature. Kerogen PAN1 is an ideal target given that it underwent a mild-thermal alteration in comparison to other studied Archean OM (Delarue et al., 2016). The degree of MDF of Xe trapped in kerogen PAN1 suggests that Archean organic materials at least  $3.0 \pm 0.3$  Gy-old are present in this 3.46 Gyr-old sample. However, the analysis of another aliquot from the same sample (PAN1b) shows no evidence for the presence of an Archean Xe component, indicating that ancient Xe isotope signatures may be heterogeneously distributed within the sample. Such heterogeneity might be related to the handpicking aliquots for analysis, where more neo-formed minerals could for instance settle at the bottom of the sample holder and be concentrated when little material is left to be analyzed. This could also be in line with observed molecular and structural heterogeneities (Lepot et al., 2013) and heterogeneous elemental distribution of noble gases in this sample. Interestingly, the  $^{40}\text{Ar}/^{36}\text{Ar}$  of bitumen cracking below  $200^\circ\text{C}$  in this kerogen are very high ( $\sim 2640$ ; Fig. 1), indicating that thermolabile materials in PAN1 are probably ancient in line with Raman spectra determined on residual bitumen droplets (Delarue et al., 2018). However, providing accurate dating of these bituminous materials in PAN1 would require knowing their mass fraction in the sample and K contents, which is not the case.

One way of potentially circumventing issues related to the occurrence of multiple generations of OM within a given sample may be to separate them based on their thermal sensitivities, as illustrated by Rock Eval studies (Delarue et al., 2018). For instance, the Rock Eval signature of kerogen MGTKS1 is largely dominated by organic materials cracking before  $400^\circ\text{C}$  (Delarue et al., 2018). This suggests that this kerogen mainly comprises thermolabile components, in line with the high H/C (Delarue et al., 2018) and absence of Archean Xe signature (this study) in this sample. Yet, several studies have argued for the presence of syngenetic organic matter in kerogen MGTKS1, notably in the form of microfossils (Sugitani et al., 2007, 2009; House et al., 2013). But since cracking of kerogen MGTKS1 releases little amounts of hydrocarbons (with respect to thermolabile organic matter, Delarue et al., 2018) and

no syngenetic Xe component, the Xe-based dating method cannot be applied. Other kerogens analyzed as part of the present study (especially 07SA22, MGTKS3 and MGTKS1up) show the release of hydrocarbons at high pyrolysis temperatures (Delarue et al., 2018), in line with the potential occurrence of ancient atmospheric Xe signatures. Whilst the multimodal release of hydrocarbons (MGTKS3 and MGTKS1up) could point towards the existence of several distinct pools of OM generating hydrocarbons at high pyrolysis temperature, the Gaussian shape of the high-temperature hydrocarbon peak detected for kerogen 07SA22 suggests a well-defined, unique generation of thermorecalcitrant organic matter in this sample. This is in line with the very consistent isotope composition of Xe extracted at  $600^\circ\text{C}$  and  $800^\circ\text{C}$ . In this case, Xe isotopes indicate that this component would not be syngenetic, but younger ( $2.3 \pm 0.1$  Gyr old) than the host rock ( $\sim 3.47$  Gyr old). Assuming kerogen 07SA22 contains a 3.47 Gyr old syngenetic component that was mixed with more recent organic materials having similar Xe concentrations but modern-like Xe isotopes would require that kerogen 07SA22 consists in 75 wt% syngenetic OM and 25 wt% modern OM. In future work, combining Rock Eval and noble gas analyses appears a promising avenue of investigation to ultimately differentiate noble gas signatures carried out by different organic components in kerogens.

## 5. Concluding remarks

The analysis of organic materials recovered from Archean rocks has the potential to elucidate on the origin of life and the timing of its emergence. Ambiguities and controversies however persist regarding the biogenetic and syngenetic origin of Archean organic materials. In particular, the potential for organic materials from ancient biological sources to co-exist with organic matter or reduced carbon produced by non-biologic processes, or post-depositional organic contaminants, suggests possible decoupling between the age of ancient organic materials and that of their host rock. Geochemical tools allowing the syngenetic origin of ancient organic materials to be tested are scarce and subject to limitations. The occurrence of non-null  $\Delta^{33}\text{S}$  values and/or  $^{129}\text{Xe}$  deficits relative to modern atmospheric composition constitute fingerprints of the Archean atmosphere. Their detection in ancient kerogens can therefore be used to validate their Archean origin. Determining the isotope composition of S within kerogens whilst limiting the contribution from associated minerals is however challenging. We recently proposed a Xe-based dating tool to potentially provide independent model ages for Archean kerogens (Bekaert et al., 2018). This method mainly relies on the combined observations that (i) atmospheric Xe evolved through time by MDF until  $\sim 2.5$  Ga (Avice et al., 2018) and (ii) ancient organic materials can preserve significant amounts of Xe trapped from the atmosphere at the time of their formation. Here, we confirm that ancient atmospheric Xe can be preserved in Archean kerogens. However, we find trapped Xe components with lower degrees of MDF than expected from the ages of the respective host rocks, raising new questions regarding the conditions allowing Xe to be efficiently trapped and preserved within ancient organic materials. We suggest that partial diffusive loss of trapped Xe is unlikely to cause such lowering of Xe degree of MDF without affecting lighter noble gases, and that multiple component mixing could more likely account for Xe-based model ages being lower than expected from the ages of host rocks. In this case, deconvoluting Xe signals from the different generations of organic matter appears extremely challenging, potentially calling for new analytical developments coupling *in situ* laser ablation techniques with an ultrasensitive mass spectrometry, and/or investigations of the thermal sensitivity of organic materials through Rock Eval studies. Before being able to tackle the question of ancient organic material syngenecity based on the Xe dating tool, it appears that a better understanding of the mechanism(s)/conditions accounting for noble gas incorporation/mobility in organic materials is needed. Moreover, these might vary depending on the geological history of the samples (e.g., temperature, extent of hydrothermalism) as well as the nature and molecular/structural composition of the organic

materials. In other words, the degree of MDF of Xe isotopes constitutes a promising – but not unequivocal – geochemical tool for providing model ages for Archean kerogens.

### Declaration of Competing Interest

The authors declare that they have no known competing financial interests or personal relationships that could have appeared to influence the work reported in this paper.

### Acknowledgments

This study was supported by the European Research Council (grants PaleoNanoLife 2011-ADG\_20110209 to F.R. and PHOTONIS 695618 to B.M.). We thank the two anonymous reviewers for their helpful comments, as well as Frances Westall for having provided the Middle Marker sample from the Barberton Greenstone Belt. We gratefully thank Raymond Michels and Laurette Piani for providing us with some bulk rock of the bituminous laminites of Orbnagou, and some IOM from the meteorite GRO 95502, respectively. This is CRPG contribution n°2727.

### Appendix A. Supplementary data

Supplementary data to this article can be found online at <https://doi.org/10.1016/j.precamres.2019.105505>.

### References

- Alexander, C.O.D., Fogel, M., Yabuta, H., Cody, G.D., 2007. The origin and evolution of chondrites recorded in the elemental and isotopic compositions of their macromolecular organic matter. *Geochim. Cosmochim. Acta* 71 (17), 4380–4403.
- Alleon, J., Bernard, S., Le Guillou, C., Beyssac, O., Sugitani, K., Robert, F., 2018. Chemical nature of the 3.4 Ga Strelley Pool microfossils. *Geochim. Perspect. Lett.* 7, 37–42.
- Allwood, A.C., Walter, M.R., Kamber, B.S., Marshall, C.P., Burch, I.W., 2006. Stromatolite reef from the Early Archean era of Australia. *Nature* 441 (7094), 714.
- Allwood, A.C., Kamber, B.S., Walter, M.R., Burch, I.W., Kanik, I., 2010. Trace elements record depositional history of an Early Archean stromatolitic carbonate platform. *Chem. Geol.* 270 (1–4), 148–163.
- Armstrong, R.A., Compston, W., De Wit, M.J., Williams, I.S., 1990. The stratigraphy of the 3.5–3.2 Ga Barberton Greenstone Belt revisited: a single zircon ion microprobe study. *Earth Planet. Sci. Lett.* 101 (1), 90–106.
- Avicé, G., Marty, B., Burgess, R., 2017. The origin and degassing history of the Earth's atmosphere revealed by Archean xenon. *Nat. Commun.* 8, 15455.
- Avicé, G., Marty, B., Burgess, R., Hofmann, A., Philippot, P., Zahnle, K., Zakharov, D., 2018. Evolution of atmospheric xenon and other noble gases inferred from Archean to Paleoproterozoic rocks. *Geochim. Cosmochim. Acta* 232, 82–100.
- Bekaert, D.V., Broadley, M.W., Delarue, F., Avicé, G., Robert, F., Marty, B., 2018. Archean kerogen as a new tracer of atmospheric evolution: implications for dating the widespread nature of early life. *Sci. Adv.* 4 (2), eaar2091.
- Bell, E.A., Boehnke, P., Harrison, T.M., Mao, W.L., 2015. Potentially biogenic carbon preserved in a 4.1 billion-year-old zircon. *Proc. Natl. Acad. Sci.* 112 (47), 14518–14521.
- Bontognali, T.R., Sessions, A.L., Allwood, A.C., Fischer, W.W., Grotzinger, J.P., Summons, R.E., Eiler, J.M., 2012. Sulfur isotopes of organic matter preserved in 3.45-billion-year-old stromatolites reveal microbial metabolism. *Proc. Natl. Acad. Sci.* 109 (38), 15146–15151.
- Bourbin, M., Derenne, S., Gourier, D., Rouzaud, J.N., Gautret, P., Westall, F., 2012. Electron paramagnetic resonance study of a photosynthetic microbial mat and comparison with Archean cherts. *Orig. Life Evol. Biosph.* 42, 569–585.
- Boussafir, M., Gelin, F., Lallier-Verges, E., Derenne, S., Bertrand, P., Largeau, C., 1995. Electron microscopy and pyrolysis of kerogens from the Kimmeridge Clay Formation, UK: source organisms, preservation processes, and origin of microcycles. *Geochim. Cosmochim. Acta* 59 (18), 3731–3747.
- Bowring, S.A., Williams, I.S., 1999. Priscoan (4.00–4.03 Ga) orthogneisses from northwestern Canada. *Contrib. Miner. Petrol.* 134 (1), 3–16.
- Cosmidis, J., Templeton, A.S., 2016. Self-assembly of biomorphic carbon/sulfur microstructures in sulfidic environments. *Nat. Commun.* 7, 12812.
- Damsté, J.S.S., De Leeuw, J.W., 1990. Analysis, structure and geochemical significance of organically-bound sulphur in the geosphere: state of the art and future research. *Org. Geochem.* 16 (4–6), 1077–1101.
- De Gregorio, B.T., Sharp, T.G., 2006. The structure and distribution of carbon in 3.5 Ga Apex chert: implications for the biogenicity of Earth's oldest putative microfossils. *Am. Mineral.* 91 (5–6), 784–789.
- Delarue, F., Rouzaud, J.N., Derenne, S., et al., 2016. The Raman-derived carbonization continuum: a tool to select the best preserved molecular structures in Archean kerogens. *Astrobiology* 16 (6), 407–417.
- Delarue, F., Derenne, S., Sugitani, K., et al., 2018. What is the meaning of hydrogen-to-carbon ratio determined in Archean organic matter? *Org. Geochem.* 122, 140–146.
- Derenne, S., Robert, F., Skrzypczak-Bonduelle, A., Gourier, D., Binet, L., Rouzaud, J.N., 2008. Molecular evidence for life in the 3.5 billion year old Warrawoona chert. *Earth Planet. Sci. Lett.* 272 (1–2), 476–480.
- Farquhar, J., Bao, H., Thiemens, M., 2000. Atmospheric influence of Earth's earliest sulfur cycle. *Science* 289 (5480), 756–758.
- French, K.L., Hallmann, C., Hope, J.M., et al., 2015. Reappraisal of hydrocarbon biomarkers in Archean rocks. *Proc. Natl. Acad. Sci.* 112 (19), 5915–5920.
- Gao, X., Thiemens, M.H., 1993a. Isotopic composition and concentration of sulfur in carbonaceous chondrites. *Geochim. Cosmochim. Acta* 57 (13), 3159–3169.
- Garcette-Lepecq, A., Derenne, S., Largeau, C., Bouloubassi, I., Saliot, A., 2000. Origin and formation pathways of kerogen-like organic matter in recent sediments off the Danube delta (northwestern Black Sea). *Org. Geochem.* 31 (12), 1663–1683.
- Gilmour, J.D., Turner, G., 1994. The RELAX mass spectrometer and its application to iodine-xenon dating. In: *Noble Gas Geochemistry and Cosmochemistry*. Terra Scientific Publishing, pp. 11–22.
- Gao, X., Thiemens, M.H., 1993b. Variations of the isotopic composition of sulfur in enstatite and ordinary chondrites. *Geochim. Cosmochim. Acta* 57 (13), 3171–3176.
- García-Ruiz, J.M., Hyde, S.T., Carnerup, A.M., Christy, A.G., Van Kranendonk, M.J., Welham, N.J., 2003. Self-assembled silica-carbonate structures and detection of ancient microfossils. *Science* 302 (5648), 1194–1197.
- Grossman, J.N., Brearley, A.J., 2005. The onset of metamorphism in ordinary and carbonaceous chondrites. *Meteorit. Planet. Sci.* 40 (1), 87–122.
- Hébrard, E., Marty, B., 2014. Coupled noble gas–hydrocarbon evolution of the early Earth atmosphere upon solar UV irradiation. *Earth Planet. Sci. Lett.* 385, 40–48.
- Horita, J., 2005. Some perspectives on isotope biosignatures for early life. *Chem. Geol.* 218 (1–2), 171–186.
- House, C.H., Oehler, D.Z., Sugitani, K., Mimura, K., 2013. Carbon isotopic analyses of ca. 3.0 Ga microstructures imply planktonic autotrophs inhabited Earth's early oceans. *Geology* 41 (6), 651–654.
- Kamber, B.S., Webb, G.E., 2001. The geochemistry of late Archean microbial carbonate: implications for ocean chemistry and continental erosion history. *Geochim. Cosmochim. Acta* 65 (15), 2509–2525.
- Konhauser, K.O., Hamade, T., Raiswell, R., Morris, R.C., Ferris, F.G., Southam, G., Canfield, D.E., 2002. Could bacteria have formed the Precambrian banded iron formations? *Geology* 30 (12), 1079–1082.
- Kuga, M., Marty, B., Marrocchi, Y., Tissandier, L., 2015. Synthesis of refractory organic matter in the ionized gas phase of the solar nebula. *Proc. Natl. Acad. Sci.* 112 (23), 7129–7134.
- Kuznetsova, A., Yates Jr, J.T., Liu, J., Smalley, R.E., 2000. Physical adsorption of xenon in open single walled carbon nanotubes: observation of a quasi-one-dimensional confined Xe phase. *J. Chem. Phys.* 112 (21), 9590–9598.
- Lee, J.Y., Marti, K., Severinghaus, J.P., Kawamura, K., Yoo, H.S., Lee, J.B., Kim, J.S., 2006. A re-determination of the isotopic abundances of atmospheric Ar. *Geochim. Cosmochim. Acta* 70 (17), 4507–4512.
- Lepland, A., van Zuilen, M.A., Arrhenius, G., Whitehouse, M.J., Fedo, C.M., 2005. Questioning the evidence for Earth's earliest life—Akilia revisited. *Geology* 33 (1), 77–79.
- Lepot, K., Williford, K.H., Ushikubo, T., Sugitani, K., Mimura, K., Spicuzza, M.J., Valley, J.W., 2013. Texture-specific isotopic compositions in 3.4 Gyr old organic matter support selective preservation in cell-like structures. *Geochim. Cosmochim. Acta* 112, 66–86.
- Lollar, B.S., Westgate, T.D., Ward, J.A., Slater, G.F., Lacrampe-Couloume, G., 2002. Abiogenic formation of alkanes in the Earth's crust as a minor source for global hydrocarbon reservoirs. *Nature* 416 (6880), 522.
- Marrocchi, Y., Marty, B., 2013. Experimental determination of the xenon isotopic fractionation during adsorption. *Geophys. Res. Lett.* 40, 4165–4170.
- Marshall, A.O., Emry, J.R., Marshall, C.P., 2012. Multiple generations of carbon in the Apex chert and implications for preservation of microfossils. *Astrobiology* 12 (2), 160–166.
- Marty, B., Altwegg, K., Balsiger, H., et al., 2017. Xenon isotopes in 67P/Churyumov-Gerasimenko show that comets contributed to Earth's atmosphere. *Science* 356 (6342), 1069–1072.
- Marty, B., Bekaert, D.V., Broadley, M.W., Jaupart, C., in press. Geochemical evidence for high volatile fluxes from the mantle at the end of the Archean. *Nature*.
- McKeegan, K.D., Kudryavtsev, A.B., Schopf, J.W., 2007. Raman and ion microscopic imagery of graphitic inclusions in apatite from older than 3830 Ma Akilia supracrustal rocks, west Greenland. *Geology* 35 (7), 591–594.
- Mojzsis, S.J., Arrhenius, G., McKeegan, K.D., Harrison, T.M., Nutman, A.P., Friend, C.R.L., 1996. Evidence for life on Earth before 3,800 million years ago. *Nature* 384 (6604), 55.
- Mongenet, T., Boussafir, M., Derenne, S., Lallier-Verges, E., Largeau, C., Tribouillard, N.P., 1997. Sulphur-rich organic matter from bituminous laminites of Orbnagou (France, upper Kimmeridgian); the role of early vulcanization. *Bulletin de la Société Géologique de France* 168 (3), 331–341.
- Oehler, D., Cady, S., 2014. Biogenicity and syngeneity of organic matter in ancient sedimentary rocks: recent advances in the search for evidence of past life. *Challenges* 5 (2), 260–283.
- Ozima, M., Podosek, F.A., 2002. Noble gas geochemistry. Cambridge University Press.
- Parai, R., Mukhopadhyay, S., 2018. Xenon isotopic constraints on the history of volatile recycling into the mantle. *Nature* 560 (7717), 223.
- Paris, G., Sessions, A.L., Subhas, A.V., Adkins, J.F., 2013. MC-ICP-MS measurement of  $\delta^{34}\text{S}$  and  $\Delta^{33}\text{S}$  in small amounts of dissolved sulfate. *Chem. Geol.* 345, 50–61.
- Paris, G., Adkins, J.F., Sessions, A.L., Webb, S.M., Fischer, W.W., 2014. Neoproterozoic carbonate-associated sulfate records positive  $\Delta^{33}\text{S}$  anomalies. *Science* 346 (6210), 739–741.

- Pavlov, A.A., Kasting, J.F., 2002. Mass-independent fractionation of sulfur isotopes in Archean sediments: strong evidence for an anoxic Archean atmosphere. *Astrobiology* 2 (1), 27–41.
- Peck, W.H., Valley, J.W., Wilde, S.A., Graham, C.M., 2001. Oxygen isotope ratios and rare earth elements in 3.3 to 4.4 Ga zircons: ion microprobe evidence for high  $\delta^{18}\text{O}$  continental crust and oceans in the Early Archean. *Geochim. Cosmochim. Acta* 65 (22), 4215–4229.
- Péron, S., Moreira, M., 2018. Onset of volatile recycling into the mantle determined by xenon anomalies. *GPL* 9, 21.
- Porcelli, D., Ballentine, C.J., 2002. An overview of noble gas geochemistry and cosmochemistry. *Rev. Mineral. Geochem.* 47, 1–19.
- Pujol, M., Marty, B., Burgess, R., 2011. Chondritic-like xenon trapped in Archean rocks: a possible signature of the ancient atmosphere. *Earth Planet. Sci. Lett.* 308 (3–4), 298–306.
- Raven, M.R., Sessions, A.L., Adkins, J.F., Thunell, R.C., 2016. Rapid organic matter sulfuration in sinking particles from the Cariaco Basin water column. *Geochim. Cosmochim. Acta* 190, 175–190.
- Rosing, M.T., 1999.  $^{13}\text{C}$ -depleted carbon microparticles in > 3700-Ma sea-floor sedimentary rocks from West Greenland. *Science* 283 (5402), 674–676.
- Saunders, M., Cross, R.J., Jiménez-Vázquez, H.A., Shimshi, R., Khong, A., 1996. Noble gas atoms inside fullerenes. *Science* 271 (5256), 1693–1697.
- Schopf, J.W., 1993. Microfossils of the Early Archean Apex chert: new evidence of the antiquity of life. *Science* 260 (5108), 640–646.
- Shen, Y., Farquhar, J., Masterson, A., Kaufman, A.J., Buick, R., 2009. Evaluating the role of microbial sulfate reduction in the early Archean using quadruple isotope systematics. *Earth Planet. Sci. Lett.* 279, 383–391.
- Simonyan, V.V., Johnson, J.K., Kuznetsova, A., Yates Jr, J.T., 2001. Molecular simulation of xenon adsorption on single-walled carbon nanotubes. *J. Chem. Phys.* 114 (9), 4180–4185.
- Spangenberg, J.E., Frimmel, H.E., 2001. Basin-internal derivation of hydrocarbons in the Witwatersrand Basin, South Africa: evidence from bulk and molecular  $\delta^{13}\text{C}$  data. *Chem. Geol.* 173 (4), 339–355.
- Sugahara, H., Sugitani, K., Mimura, K., Yamashita, F., Yamamoto, K., 2010. A systematic rare-earth elements and yttrium study of Archean cherts at the Mount Goldsworthy greenstone belt in the Pilbara Craton: implications for the origin of microfossil-bearing black cherts. *Precamb. Res.* 177 (1–2), 73–87.
- Sugitani, K., Grey, K., Allwood, A., et al., 2007. Diverse microstructures from Archaean chert from the Mount Goldsworthy-Mount Grant area, Pilbara Craton, Western Australia: microfossils, dubiofossils, or pseudofossils? *Precamb. Res.* 158 (3–4), 228–262.
- Sugitani, K., Grey, K., Nagaoka, T., Mimura, K., Walter, M.R., 2009. Taxonomy and biogenicity of Archaean spheroidal microfossils (ca. 3.0 Ga) from the Mount Goldsworthy-Mount Grant area in the northeastern Pilbara Craton, Western Australia. *Precamb. Res.* 173 (1–4), 50–59.
- Sugitani, K., Mimura, K., Nagaoka, T., Lepot, K., Takeuchi, M., 2013. Microfossil assemblage from the 3400 Ma Strelley Pool Formation in the Pilbara Craton, Western Australia: results form a new locality. *Precamb. Res.* 226, 59–74.
- Tashiro, T., Ishida, A., Hori, M., et al., 2017. Early trace of life from 3.95 Ga sedimentary rocks in Labrador, Canada. *Nature* 549 (7673), 516.
- Thorpe, R.I., Hickman, A.H., Davis, D.W., Mortensen, J.K., Trendall, A.F., 1992. Constraints to models for Archean lead evolution from precise zircon U-Pb geochronology for the Marble Bar region, Pilbara Craton, Western Australia. In: Glover, J.E., Ho, S.E. (Eds.), *The Archean: Terrains, Processes and Metallogeny*. Univ. West. Austral. Geol. Extens. Publ. 22, pp. 395–407.
- Torgersen, T., Kennedy, B.M., van Soest, M.C., 2004. Diffusive separation of noble gases and noble gas abundance patterns in sedimentary rocks. *Earth Planet. Sci. Lett.* 226 (3–4), 477–489.
- Van Zuilen, M.A., Lepland, A., Arrhenius, G., 2002. Reassessing the evidence for the earliest traces of life. *Nature* 418 (6898), 627.
- Wacey, D., Kilburn, M.R., Saunders, M., Cliff, J., Brasier, M.D., 2011. Microfossils of sulphur-metabolizing cells in 3.4-billion-year-old rocks of Western Australia. *Nat. Geosci.* 4 (10), 698.
- Wacker, J.F., Zadnik, M.G., Anders, E., 1985. Laboratory simulation of meteoritic noble gases. I. Sorption of xenon on carbon: trapping experiments. *Geochim. Cosmochim. Acta* 49 (4), 1035–1048.
- Wacker, J.F., 1989. Laboratory simulation of meteoritic noble gases. III. Sorption of neon, argon, krypton, and xenon on carbon: elemental fractionation. *Geochim. Cosmochim. Acta* 53 (6), 1421–1433.
- Walter, M.R., Buick, R., Dunlop, J.S.R., 1980. Stromatolites 3400–3500 Myr old from the North pole area, Western Australia. *Nature* 284 (5755), 443.
- Warr, O., Lollar, B.S., Fellowes, J., et al., 2018. Tracing ancient hydrogeological fracture network age and compartmentalisation using noble gases. *Geochim. Cosmochim. Acta* 222, 340–362.
- Watanabe, Y., Farquhar, J., Ohmoto, H., 2009. Anomalous fractionations of sulfur isotopes during thermochemical sulfate reduction. *Science* 324 (5925), 370–373.
- Westall, F., de Wit, M.J., Dann, J., van der Gaast, S., de Ronde, C.E., Gerneke, D., 2001. Early Archean fossil bacteria and biofilms in hydrothermally-influenced sediments from the Barberton greenstone belt, South Africa. *Precamb. Res.* 106 (1–2), 93–116.
- Wilde, S.A., Valley, J.W., Peck, W.H., Graham, C.M., 2001. Evidence from detrital zircons for the existence of continental crust and oceans on the Earth 4.4 Gyr ago. *Nature* 409 (6817), 175.
- Yang, J., Lewis, R.S., Anders, E., 1982. Sorption of noble gases by solids, with reference to meteorites. I: magnetite and carbon. *Geochim. Cosmochim. Acta* 46, 841–860.
- Zahnle, K.J., Gacesa, M., Catling, D.C., 2019. Strange messenger: a new history of hydrogen on Earth, as told by Xenon. *Geochim. Cosmochim. Acta* 244, 56–85.